International Urology and Nephrology (2019) 51:425–434
https://doi.org/10.1007/s11255-019-02083-8

UROLOGY - ORIGINAL PAPER

Whole mount histopathological correlation with prostate MRI in Grade I and II prostatectomy patients

Michael Wang[1,3] · Nafiseh Janaki[2] · Christina Buzzy[1,3] · Laura Bukavina[1] · Amr Mahran[1,3] · Kirtishri Mishra[1] · Gregory MacLennan[2] · Lee Ponsky[1,3]

Received: 23 November 2018 / Accepted: 17 January 2019 / Published online: 22 January 2019

Abstract

Background Multiparametric magnetic resonance imaging (mpMRI) is increasingly used in detection and surveillance of prostate cancer. However, the co-localization of lower grade lesions between mpMRI and histopathologic specimen has not been well established.

Objective We aim to determine the factors on final histopathological exam that correlate to tumor visibility for Grade I and II disease on mpMRI.

Methods Fifty-five patients who underwent radical prostatectomy from July 2014 to June 2016 were analyzed for the study. Of the sample of 55 patients, 18 were found to have Gleason score (GS) of 3 + 3 or 3 + 4 disease, and then were re-reviewed and annotated by a pathologist. Lesion diameter, area, and distance from the prostate capsule were measured. The annotated lesions were co-localized to the MRI report.

Results Of the 184 lesions identified on the whole mount histopathologic slides, 106 (57.6%), 62 (33.7%), 14 (7.6%), and 2 (1.1%) of the lesions had a GS of 3 + 3, 3 + 4, 4 + 3, and 4 + 4, respectively. On analysis, 27.3% (24/88) of GS 6 (< 1.5 cm in size), and 88.9% (16/18) of GS 6 (> 1.5 cm in size) were identified ($p < 0.001$). Additionally, when assessing lesion proximity to the prostatic capsule, 46.1% (41/89) of lesions closer (≤ 0.05 cm), and 30.5% (29/95) of lesions further (> 0.05 cm) from the capsule were visualized.

Conclusion Lesion diameter, area, and capsule proximity correlated with MRI visibility. Further studies are encouraged to validate the findings of our study.

Keywords Multiparametric MRI · Prostate cancer · Intermediate prostate cancer · Histopathology

Introduction

Multiparametric magnetic resonance imaging (mpMRI) has considerable value in detection of clinically significant prostate cancer while minimizing over-detection of indolent disease. Despite advances in MRI over the last several years, confirmatory biopsy of insignificant lesions on MRI may still reveal intermediate- or high-risk disease. Central dogma of MR imaging lies in continuous improvement of MRI interpretation, as well as more accurate correlation with whole mount histopathology [1].

As previously described in the literature, index lesion size, tumor volume, biopsy Gleason grade, glandular architecture, and tumor location all correlate with lesion visibility on MRI [1–4]. Despite mounting evidence on factors listed previously, little research has been dedicated to assess the features responsible for MRI visibility for Grade I and II disease.

Electronic supplementary material The online version of this article (https://doi.org/10.1007/s11255-019-02083-8) contains supplementary material, which is available to authorized users.

✉ Lee Ponsky
Lee.Ponsky@UHhospitals.org

[1] Division of Urologic Oncology, Urology Institute, University Hospitals Cleveland Medical Center, 11100 Euclid Avenue, Cleveland, OH 44106, USA

[2] Department of Pathology, University Hospitals Cleveland Medical Center, Cleveland, OH, USA

[3] Case Western Reserve University School of Medicine, Cleveland, OH, USA

In the current study, we examine the histopathologic characteristics in Grade I and II disease associated with MRI detection. We aim to compare the findings on mpMRI with the histopathologic findings from the radical prostatectomy (RP) specimen, and to evaluate pathologic factors responsible for MR visibility in Grade I and II disease.

Methods

Study population and imaging

An IRB-approved retrospective study was conducted for patients who had an MRI prior to prostatectomy from July 2014 to June 2016 at our institution. From a representative sample of 55 patients, 18 patients were found to have GS of 3 + 3 or 3 + 4 disease. Patient encounters, radiologic, and histopathologic reports were examined retrospectively from the institution's electronic medical records.

All patients underwent mpMRI using a 3.0-T unit MRI (Verio or Skyra, Siemens Healthineers). The MRI scans were read and scored by one of five expert radiologists, with an average experience of 15 years, utilizing the European Society of Urogenital Radiology (ESUR) PI-RADS v1 (prior to 2014) or v2 (after 2015) scoring system [5]. PI-Evaluation using RADS v1 and PI-RADS v2 has previously been evaluated, with studies showing no difference in diagnostic accuracy [4]. PI-RADS 1 and 2 lesions, according to the American College of Radiology Guidelines, are unlikely to harbor clinically significant cancer [5, 6]. In this study, lesions given a PI-RADS of 1 or 2 were defined as not visible, whereas PI-RADS 3, 4, and 5 were considered visible.

Histopathologic analysis and co-localization

Whole mount prostatectomy specimens were sliced in 3–5-mm increments. A pathologist (N.J) blinded to the MRI and pathology results re-reviewed all prostatectomy slides. Annotated whole mount slides from RP specimens were individually digitized and each lesion was measured using AdobeAcrobat (supplementary). The lesion diameter (longest axis), lesion area, distance to prostatic capsule, and ratio of tumor to total area were all measured and documented. Cancerous lesions that were of the same Gleason grade and were within 1.5 mm of each other were considered part of the same lesion. Lesions on each slide were counted non-contiguously and evaluated separately from other mount prostatectomy slides.

Lesion size and location were correlated between the MRI and the pathologic specimen. Lesion ratio was defined as the area of the lesion in question to whole mount area. Lesions listed in the MRI report had to be in the same zone, segment, and axis as the whole mount slide for it to be characterized as *identified*. Continuous lesions across multiple whole mount slides were characterized as one, and if they correlated with a MRI lesion, then they were documented as a single *identified* lesion. Furthermore, a PI-RADS score of at least 3 was needed for the *identified* lesion to be characterized as *visible*. Lesions re-annotated on the prostatectomy whole mount slices were the reference standard and were considered false negative if not identified on the MRI.

Index lesions in multifocal specimen were classified according to one of the two definitions: (1) lesions with extracapsular extension (ECE), highest Gleason score, and largest tumor size (standard definition), and (2) tumors with the largest diameter.

Statistical analysis

All data were analyzed using RStudio (RStudio, Inc). Categorical data were presented as counts and relative

Table 1 Patient demographics

Patient characteristics			Value
Age			61.4 (57.6–66.1)
PSA* (ng/mL)			5.8[a] (4.8–9.9)
Prostate weight (g)			43.3 (35.0–51.5)
Prostate volume (cm^3)			36.0 (26.2–38.3)
Final histopathology Gleason Score			
3 + 3			4 (22.2%)
3 + 4			14 (77.8%)
Final histopathology lesion number			184
Gleason Score, number of lesions			
3 + 3			106 (57.6%)
3 + 4			62 (33.7%)
4 + 3			14 (7.6%)
4 + 4			2 (1.1%)
Pathologic stage			
T2a			1
T2b			0
T2c			10
T3a			4
T3b			3
	Not visualized on MRI	Visualized on MRI	*p* value
N	5	4	
PSA* total (median [IQR])	4.80 [4.77, 5.58]	10.95 [9.58, 13.23]	0.027

Continuous variables: mean (IQR), categorical variables: *n* (%)

PSA prostate-specific antigen

*PSA differences compared via Mann Whitney U test between lesions visualized and not visualized on MRI (10 patients experienced both)

[a]Median

Table 2 Characteristics of prostate lesions and tumor detection ($n=184$) by mpMRI

Characteristics	Positive MRI findings and positive histopathologic results ($n=70$)	Negative MRI findings and positive histopathologic results ($n=114$)	p
Index tumor status (grade)			< 0.05
Index tumor	27 (55.1%)	22 (44.9%)	
Non-index tumor	43 (31.9%)	92 (68.1%)	
Index tumor status (size)			< 0.001
Index tumor	41 (65.1%)	22 (34.9%)	
Non-index tumor	29 (24.0%)	92 (76%)	
Tumor diameter			< 0.001
≤ 0.5 cm	7 (22.6%)	24 (77.4%)	
0.5–1.0 cm	11 (19.0%)	47 (81.0%)	
1.0–1.5 cm	14 (35.0%)	26 (65.0%)	
1.5–3.0 cm	32 (65.3%)	17 (34.7%)	
> 3 cm	6 (100%)	0 (0%)	
Gleason Score			0.98
3 + 3	40 (37.7%)	66 (62.3%)	
3 + 4	24 (38.7%)	38 (61.3%)	
4 + 3	5 (35.7%)	9 (64.3%)	
4 + 4	1 (50%)	1 (50%)	
Total	70 (38%)	114 (62%)	

Table 3 Prostate lesion size, area, and tumor detection by MRI, stratified by Gleason Score

	Positive MRI findings and positive histopathologic results	Negative MRI findings and positive histopathologic results	p		Positive MRI findings and positive histopathologic results	Negative MRI findings and positive histopathologic results	p
Lesion size (cm)				Lesion area (cm^2)			
Gleason Score 3 + 3			< 0.001	Gleason Score 3 + 3			< 0.001
≤ 0.5	7 (28%)	18 (72%)		≤ 0.1	6 (28.6%)	15 (71.4%)	
0.5–1.0	9 (20.9%)	34 (79.1%)		0.1–0.5	13 (22.4%)	45 (77.6%)	
1.0–1.5	8 (40%)	12 (60%)		0.5–1.0	9 (64.3%)	5 (35.7%)	
1.5–3	15 (88.2%)	2 (11.8%)		1.0–1.5	6 (85.7%)	1 (14.3%)	
> 3	1 (100%)	0 (0%)		> 1.5	6 (100%)	0 (0%)	
Subtotal	40 (57.1%)	66 (57.9%)		Subtotal	40 (57.1%)	66 (57.9%)	
Gleason Score > 3 + 4			< 0.001	Gleason Score > 3 + 4			< 0.001
≤ 0.5	0 (0%)	6 (100%)		≤ 0.1	0 (0%)	7 (100%)	
0.5–1.0	2 (13.3%)	13 (86.7%)		0.1–0.5	4 (20.0%)	16 (80.0%)	
1.0–1.5	6 (30.0%)	14 (70.0%)		0.5–1.0	4 (22.2%)	14 (77.8%)	
1.5–3	17 (53.1%)	15 (46.9%)		1.0–1.5	9 (56.3%)	7 (43.7%)	
> 3	5 (100%)	0 (0%)		> 1.5	13 (76.5%)	4 (23.5%)	
Subtotal	30 (42.9%)	48 (42.1%)		Subtotal	30 (42.9%)	48 (42.1%)	
Total	70 (38%)	114 (62%)		Total	70 (38%)	114 (62%)	

frequencies. Continuous variables were described using the mean for normally distributed data and median for non-normally distributed data, followed by interquartile ranges (IQR). Further stratifications for index lesions, lesion size and area, distance to capsule, and lesion ratios were conducted based on GS (6 vs. > 6) and lesion diameter (median = 1.07 cm). Student's t test and chi-squared analysis were utilized for continuous and categorical variables, respectively. A p value less than 0.05 indicated statistical significance.

Results

Patient characteristics are depicted in Table 1. Overall, the mean age of the study group was 61.4 years old (SD 57.6–66.1) at RP, median PSA of 5.8 ng/ml (IQR 4.8–9.9), median prostate and seminal vesicle weight of 43.3 g (IQR 35.0–51.5 g), and median prostate volume of 36 cm^3 (IQR 26.2–38.3 cm^3) on RP (Table 1). Of the 184 lesions identified on the whole mount slides, 106 (57.6%), 62 (33.7%), 14 (7.6%), and 2 (1.1%) of the lesions had a GS of 3 + 3, 3 + 4, 4 + 3, and 4 + 4, respectively.

Out of 184 lesions, 70 (38%) were visualized on MRI (Table 2). When definition 1 (ECE, GS, and tumor diameter) was used to identify the index, MRI detected 55.1% (27/49) of the index lesions and 31.9% (43/135) of the non-index lesions ($p < 0.05$). When definition 2 (largest diameter) was used to define the index lesion, 41/63 (65.1%) of the index and 22/63 (34.9.0%) of the non-index lesions were detected ($p < 0.001$).

When comparing PSA differences among patients with lesions visualized on MRI in both Grade I and II disease, as compared to lesions not seen on MRI, differences were noted. Median PSA of visualized lesions was 10.95 [IQR 9.58, 13.23], as compared to 4.80 [IQR 4.77, 5.58], $p = 0.027$ (Table 1).

The median lesion size was 1.23 cm (IQR 0.59–1.78). Of the 129 lesions less than or equal to 1.5 cm in diameter, based on RP final pathology, 24.8% (32/129) were detected

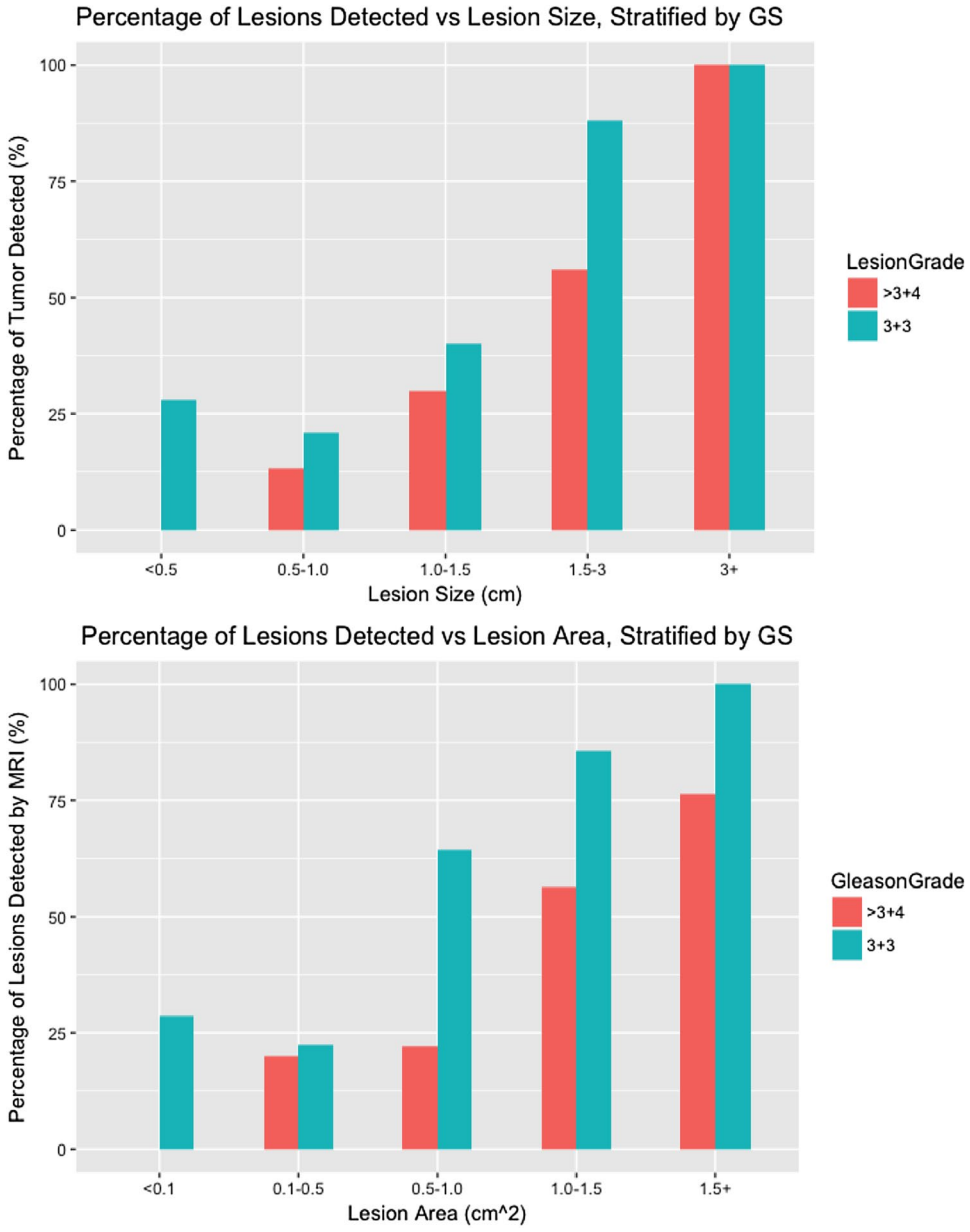

Fig. 1 Percentage of Lesions Detected on MRI stratified by Lesion Size and Gleason score

Table 4 Distance of lesions to prostatic capsule and tumor detection ($n=184$) by mpMRI, stratified by Gleason score and lesion size

	Positive MRI findings and positive histopathologic results	Negative MRI findings and positive histopathologic results	*p*
All lesions			
Distance to capsule (cm)			< 0.05
≤ 0.05	41 (46.1%)	48 (53.9%)	
0.05–0.10	6 (30.0%)	14 (70.0%)	
0.1–0.2	8 (29.6%)	19 (70.4%)	
0.2–0.5	12 (36.4%)	21 (63.6%)	
0.5+	3 (16.7%)	12 (83.3%)	
Total	70 (38%)	114 (62%)	
Lesion size ≤ 1.07 (cm)			0.724
Distance to capsule (cm)			
≤ 0.05	5 (17.9%)	23 (82.1%)	
0.05–0.10	2 (18.2%)	9 (81.8%)	
0.1–0.2	1 (7.14%)	13 (92.9%)	
0.2–0.5	8 (32.0%)	17 (68.0%)	
0.5+	3 (23.1%)	10 (76.9%)	
Lesion size > 1.07 (cm)			0.101
Distance to capsule (cm)			
≤ 0.05	36 (59.0%)	25 (61%)	
0.05–0.10	4 (44.4%)	5 (55.6%)	
0.1–0.2	7 (53.8%)	6 (46.2%)	
0.2–0.5	4 (50%)	4 (100%)	
0.5+	0 (0.0%)	2 (100%)	
Total	70 (38%)	114 (62%)	
Gleason 3 + 3			
Distance to capsule (cm)			0.296
≤ 0.05	19 (41.3%)	27 (58.7%)	
0.05–0.10	4 (30.8%)	9 (69.2%)	
0.1–0.2	6 (35.3%)	11 (64.7%)	
0.2–0.5	8 (42.1%)	11 (57.9%)	
0.5+	3 (27.3%)	8 (72.7%)	
Gleason > 3 + 4			< 0.001
Distance to capsule (cm)			
≤ 0.05	22 (53.5%)	21 (46.5%)	
0.05–0.10	2 (28.6%)	5 (71.4%)	
0.1–0.2	2 (20%)	8 (80%)	
0.2–0.5	4 (28.6%)	10 (71.4%)	
0.5+	0 (0.0%)	4 (100%)	
Total	70 (38%)	114 (62%)	

on prostate MRI. Of the remaining 55 lesions greater than 1.5 cm, 69.1% (38/55) were identified on MRI (Table 2). Of the 106 lesions with a GS 6, 37.7% (40/106) and 38.5% (30/78) of GS ≥ 7 of the lesions were identified on MRI ($p=0.98$).

On further analysis, 27.3% (24/88) of GS 6 (< 1.5 cm in size), and 88.9% (16/18) of GS 6 (> 1.5 cm in size) were identified ($p<0.001$) (Table 3). Eight of forty-one lesions with Gleason ≥ 7 (19.5%) measuring less than 1.5 cm in diameter were detected on the MRI, whereas 67.6% (22/37) of lesions measuring greater than 1.5 cm were visualized ($p<0.001$). As evidenced in Table 3, Gleason 6 with area of less than 0.5 cm^2 were missed 60/79 (75.9%) on MRI imaging, whereas 21/27 (77.8%) of those greater than 0.5 cm^2 were detected ($p<0.001$) (Fig. 1).

When assessing MRI lesion visibility according to proximity of the lesion to the prostatic capsule, 46.1% (41/89) of lesions closer (≤ 0.05 cm) to the prostatic capsule were visualized, and 30.5% (29/95) of lesions further from the capsule (> 0.05 cm) were visualized (Table 4). Additional subgroup

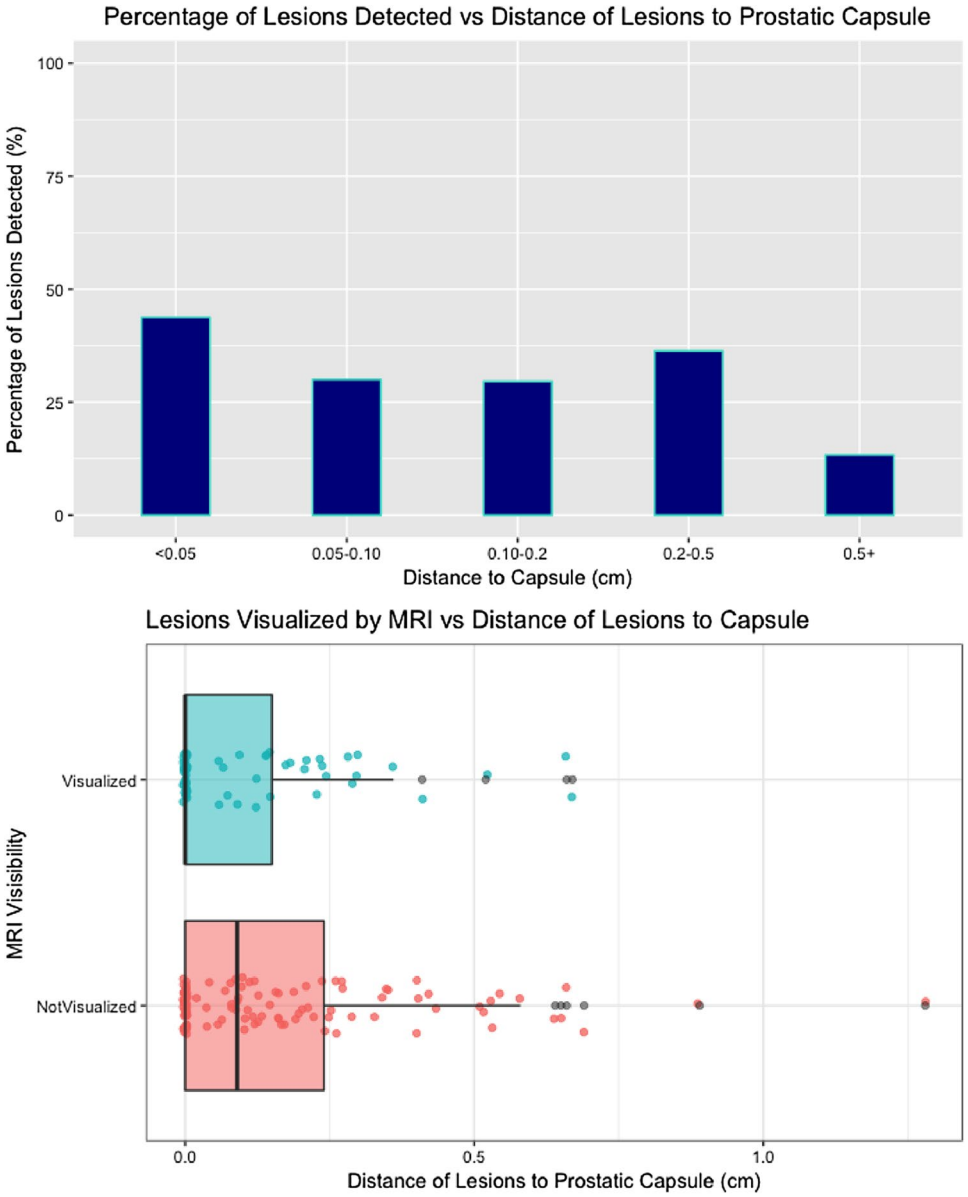

Fig. 2 Percentage of Lesions Detected on MRI stratified by distance of the lesion to the prostatic capsule

analysis using lesion Gleason grade (GS 6 or GS > 6) with distance to capsule displayed no statistical difference of lesions from prostatic capsule for GS 6 lesions ($p = 0.296$). For lesions with a GS > 6, 51.2% (22/43) of the lesions less than 0.05 cm from the capsule were visualized, whereas 8/35 (22.9%) of the lesions were seen for those greater than 0.05 cm ($p < 0.001$) (Fig. 2).

Twenty-nine percent (41/140) of lesion ratios less than 10% were visualized, whereas 65.9% (29/44) of lesion ratios greater than 10% were visualized ($p < 0.001$) (Table 5).

When stratified by the median lesion size (1.07 cm), lesion ratios for lesion sizes less than 1.07 cm displayed no statistically significant relationship with prostate MRI visibility ($p = 0.52$). However, for lesion sizes greater than 1.07 cm, 44% (22/50) of lesion ratios less than 10% were visualized when compared to 29/43 (67.4%) of lesion ratios greater than 10% ($p < 0.01$) (Fig. 3).

Discussion

Studies evaluating index tumors have shown correlation between the index lesion and progression of prostatic malignancy. Thus, identification of index lesion on mpMRI can aid in planning surgical and radiation treatments [7, 8]. In our study, MRI detected 55.1% of index lesions when using the "standard definition" of index lesion [1]. When using lesion size as the definition for determining index lesions, the visibility rate rises up to 65.1%. While this is still significantly lower than past studies examining index lesions,

Table 5 mpMRI visibility vs lesion ratio stratified by histopathologic results

Lesion ratio	Positive MRI findings and positive histopathologic results	Negative MRI findings and positive histopathologic results	*p*	Lesion ratio	Positive MRI findings and positive histopathologic results	Negative MRI findings and positive histopathologic results	*p*
All lesions			< 0.001				
< 1%	5 (20.8%)	19 (79.2%)					
1–5%	18 (22.5%)	62 (77.5%)					
5–10%	18 (50%)	18 (50%)					
> 10%	29 (65.9%)	15 (34.1%)					
Total	70	114	184				
Gleason Score 3 + 3			< 0.001	Gleason Score > 3 + 4			< 0.001
< 1%	5 (27.8%)	13 (72.2%)		< 1%	0 (0%)	6 (100%)	
1–5%	15 (25.9%)	43 (74.1%)		1–5%	3 (13.6%)	19 (86.4%)	
5–10%	10 (58.8%)	7 (41.2%)		5–10%	8 (42.1%)	11 (57.9%)	
> 10%	10 (76.9%)	3 (23.1%)		> 10%	19 (61.3%)	12 (38.7%)	
Total	40	66			30	48	184
Lesion size < 1.07 cm			0.52	Lesion size > 1.07 cm			< 0.01
< 1%	5 (20.8%)	19 (79.2%)		< 1%	0	0	
1–5%	12 (19.0%)	51 (81%)		1–5%	6 (35.3%)	11 (64.7%)	
5–10%	2 (66.7%)	1 (33.3%)		5–10%	16 (48.5%)	17 (51.2%)	
> 10%	0 (0%)	1 (100%)		> 10%	29 (67.4%)	14 (32.6%)	
Total	19	72			51	42	184

whose sensitivities usually ranged above 90% [8–10], the low visibility rate could be attributed to the low final GS in our cohort. In our study, we found the visibility on the MRI to be dominated primarily by the larger size of the lesion rather than by the highest Gleason score within the lesion. As index lesions are considered the leading factor in disease progression [2], the goal of MRI/US fusion biopsy is to identify these lesions so as to guide clinical decisions.

Despite overwhelming consensus that higher GS lesions lead to increased MRI sensitivity in the prospective data, retrospective review of our data did support this finding ($p = 0.98$) [1, 3]. When stratifying lesions by GS, we found no statistically significant difference between the visibility of GS6 and GS7^{+} lesions. Delongchamps et al. described all their invisible GS7 lesions on MRI as constituting a makeup of less than 20% of grade 4, especially if they were small lesions [11]. Likewise, our cohort of primarily GS 3 + 3 and GS 3 + 4 lesions demonstrated that individual Gleason scores in an overall low-grade final GS RP did not significantly impact the visibility of lesions on MRI; rather, it was the lesion size and lesion area driving the visibility.

In our study, histopathologic review revealed that lesions closer to the prostatic capsule had a higher rate of visualization on MRI. However, when we further stratified by Gleason score, only GS7^{+} showed statistical significance. Once we stratified the cohort by the median lesion size (1.07 cm), the relationship between distance to prostatic capsule for small lesions was no longer statistically significant for lesions < 1.07 cm. For larger lesions (> 1.07 cm), the association between visibility and distance to capsule approaches significance. Thus, the relationship between visibility on the mpMRI and distance of lesion to prostatic capsule may be a function of tumor size, as larger PZ tumors have often been noted to be located subcapsularly, whereas smaller PZ tumors are interspersed throughout the zone [12]. This relationship was also noted in our cohort.

Rosenkratz et al. and Panebianco et al. also noted that the periprostatic vein and neurovascular bundle can often mimic PZ lesions adjacent to the capsule—which when combined with lesions already near the capsule could make them more evident on MRI [13, 14]. This is the first study that we know of that compared the lesion visibility on mpMRI and histopathologically determined lesion distance from prostatic capsule; a larger cohort analyzing the relationship between lesion's distance to prostatic capsule to mpMRI visibility is needed.

Our study similarly examined the lesion area ratio of all lesions. As expected, increased lesion area ratio correlated with a higher MRI visibility. Once again, we stratified the lesions by the median lesion size to hold lesion size stable; nevertheless, the lesion area ratio was still positively correlated with mpMRI visibility for lesion sizes greater than 1.07 cm. This demonstrates that after accounting for lesion size, varying lesion area ratio correlated with the visibility

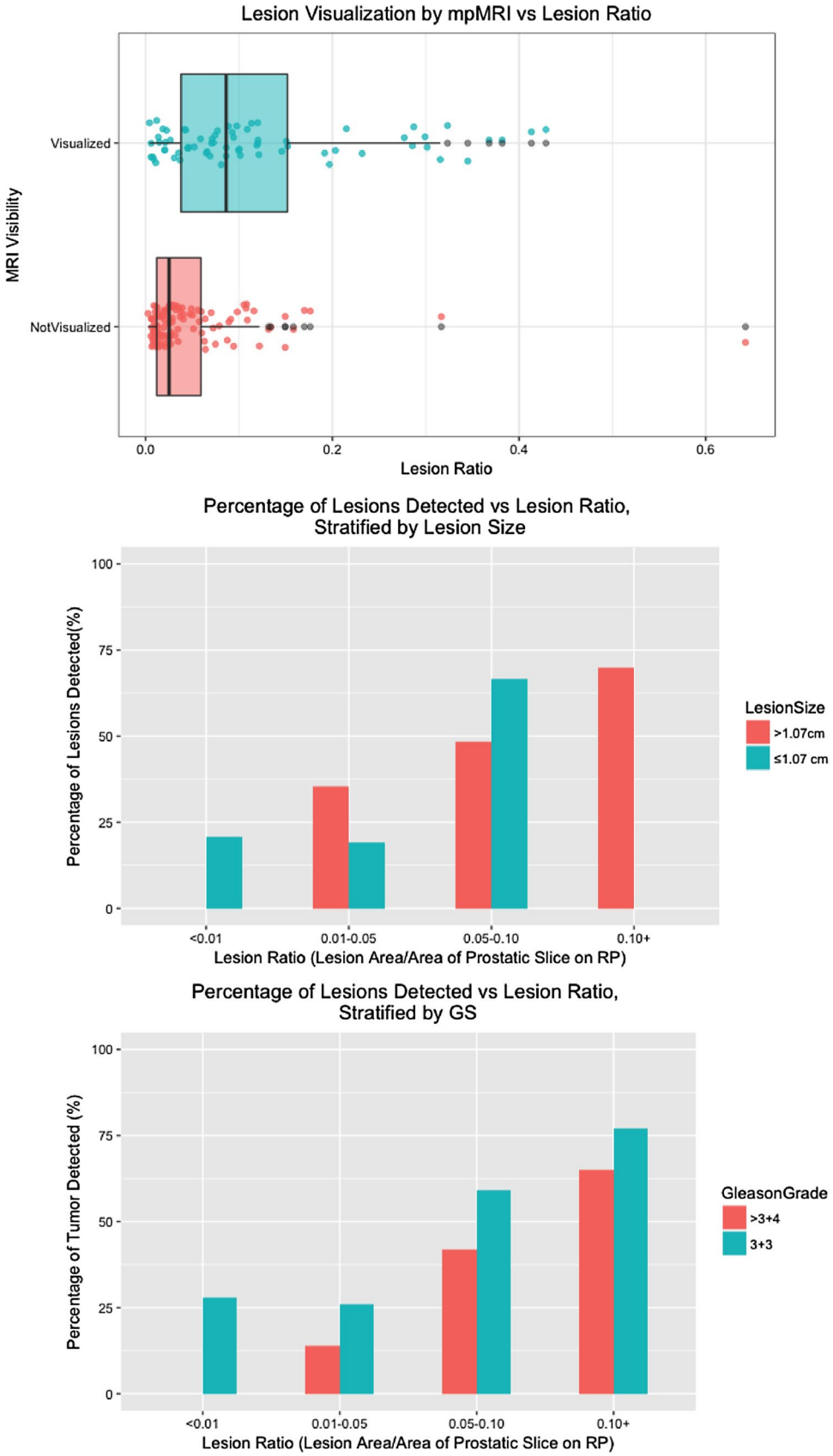

Fig. 3 **a** Lesion visualization by mpMRI vs Lesion Ratio (lesion size/whole mount) **b** Percentage of Lesions Detected vs Lesion Ratio, Stratified by Lesion Size

on the MRI. This trend has been described in past studies, where the utilization of mpMRI-US fusion biopsy on smaller prostate sizes yielded higher detection rates of clinically significant cancer when compared to larger glands [15, 16]. While mpMRI-US fusion biopsy was implemented to decrease the false-negative rate associated with a large prostate for systematic TRUS biopsy [17], it is still not clear as to why there is such a discrepancy in the cancer detection rate between varying prostate volume sizes when utilizing mpMRI-US fusion biopsy. Some studies have suggested that smaller prostates naturally harbor larger and more aggressive PCa [18–20]. Other studies attribute that phenomenon to a higher proportion of low volume cancer in large prostate leading to low detection rates upon biopsy, possibly due to lead time bias [21]. Yet, these studies do not explain the decreased visibility of lesions in large prostates on mpMRI. Patients harboring large lesions in large prostates can have intermediate-risk lesions upon biopsy but can still be missed on MRI due to low lesion area ratio—a relationship that warrants further investigation.

There are several limitations in this study, including the single-center design, MRI inter-observer variability, and accuracy of co-localization of the histopathology to the MRI. Studies have shown that with experienced readers, the reproducibility of PI-RADS scoring were similar, especially when reading the PZ [22]. In addition, we identified the lesions on histopathologic evaluation as individual, and not in contiguous manner. This provides an opportunity to perform a superior lesion analysis, although not as clinically significant.

In this analysis, we found index tumor, lesion size, lesion area, lesion area ratio, and lesion's distance to prostatic capsule to be correlated to MRI lesion visibility in prostates with Gleason score of $3+3$ or $3+4$. A higher GS was not predictive of MRI visibility in this cohort. Lesion area ratio was also predictive of MRI visibility when controlling for lesion size. These findings are first to be reported in the literature, and provide further insight to physicians in guiding prostate cancer treatment.

Conclusions

The role of mpMRI is rapidly evolving. A combined approach with histopathologic evaluation can help physicians accurately tailor individual therapy. Our study identified "risk factors" for MRI visibility of low- and intermediate-grade lesions. Further prospective research is necessary to identify factors responsible for MRI visibility of not only high- and intermediate-risk disease, but low-risk cancers as well. Moreover, research on personalized MRI fingerprinting, and risk maps, which can help identify patients at risk for clinically significant, is strongly encouraged.

References

1. Le JD, Tan N, Shkolyar E et al (2015) Multifocality and prostate cancer detection by multiparametric magnetic resonance imaging: correlation with whole-mount histopathology. Eur Urol 67:569–576
2. Russo F, Regge D, Armando E et al (2016) Detection of prostate cancer index lesions with multiparametric magnetic resonance imaging (mp-MRI) using whole-mount histological sections as the reference standard. BJU Int 118:84–94
3. Bratan F, Niaf E, Melodelima C et al (2013) Influence of imaging and histological factors on prostate cancer detection and localisation on multiparametric MRI: a prospective study. Eur Radiol 23:2019–2029
4. Becker AS, Cornelius A, Reiner CS et al (2017) Direct comparison of PI-RADS version 2 and version 1 regarding interreader agreement and diagnostic accuracy for the detection of clinically significant prostate cancer. Eur J Radiol 94:58–63
5. Barentsz JO, Weinreb JC, Verma S et al (2016) Synopsis of the PI-RADS v2 guidelines for multiparametric prostate magnetic resonance imaging and recommendations for use. Eur Urol 69:41–49
6. Weinreb JC, Barentsz JO, Choyke PL et al (2016) PI-RADS prostate imaging—reporting and data system: 2015, Version 2. Eur Urol 69:16–40
7. Liu W, Laitinen S, Khan S et al (2009) Copy number analysis indicates monoclonal origin of lethal metastatic prostate cancer. Nat Med 15:559–565
8. Turkbey B, Brown AM, Sankineni S et al (2016) Multiparametric prostate magnetic resonance imaging in the evaluation of prostate cancer. CA Cancer J Clin 66:326–336
9. Baco E, Ukimura O, Rud E et al (2015) Magnetic resonance imaging–transectal ultrasound image-fusion biopsies accurately characterize the index tumor: correlation with step-sectioned radical prostatectomy specimens in 135 patients. Eur Urol 67:787–794
10. Rud E, Klotz D, Rennesund K et al: Detection of the index tumour and tumour volume in prostate cancer using T2-weighted and diffusion-weighted magnetic resonance imaging (MRI) alone. BJU Int 114: E32–E42
11. Delongchamps NB, Lefèvre A, Bouazza N et al (2015) Detection of significant prostate cancer with magnetic resonance targeted biopsies—should transrectal ultrasound-magnetic resonance imaging fusion guided biopsies alone be a standard of care? J Urol 193:1198–1204
12. Rosenkrantz AB, Verma S, Turkbey B (2015) Prostate cancer: top places where tumors hide on multiparametric MRI. Am J Roentgenol 204:W449–W456
13. Rosenkrantz AB, Taneja SS (2015) Prostate MRI can reduce overdiagnosis and overtreatment of prostate cancer. Acad Radiol 22:1000–1006
14. Panebianco V, Barchetti F, Barentsz J et al (2015) Pitfalls in interpreting mp-MRI of the prostate: a pictorial review with pathologic correlation. Insights Imaging 6:611–630
15. de Gorski A, Rouprêt M, Peyronnet B et al (2015) Accuracy of magnetic resonance imaging/ultrasound fusion targeted biopsies to diagnose clinically significant prostate cancer in enlarged compared to smaller prostates. J Urol 194:669–673
16. Giannarini G, Crestani A, Rossanese M et al (2017) Multiparametric magnetic resonance imaging targeted biopsy for early

detection of prostate cancer: All That Glitters Is Not Gold! Eur Urol 71:904–906
17. Walton Diaz A, Hoang AN, Turkbey B et al (2013) Can magnetic resonance-ultrasound fusion biopsy improve cancer detection in enlarged prostates? J Urol 190:2020–2025
18. Zhu X, Albertsen PC, Andriole GL et al (2012) Risk-based prostate cancer screening. Eur Urol 61:652–661
19. Briganti A, Chun FK-H, Suardi N et al (2007) Prostate volume and adverse prostate cancer features: fact not artifact. Eur J Cancer 43:2669–2677
20. Freedland SJ, Isaacs WB, Platz EA et al (2005) Prostate size and risk of high-grade, advanced prostate cancer and biochemical progression after radical prostatectomy: a search database study. J Clin Oncol 23:7546–7554
21. Chen ME, Troncoso P, Johnston D et al (1999) Prostate cancer detection: relationship to prostate size. Urology 53:764–768
22. Rosenkrantz AB, Lim RP, Haghighi M et al (2013) Comparison of interreader reproducibility of the prostate imaging reporting and data system and Likert scales for evaluation of multiparametric prostate MRI. Am J Roentgenol 201:W612–W618